The Microstructure and Hardness of ZrO2 Reinforced 24CrNiMoY Alloy Prepared by SLM

Chaofan Shi[1], Suiyuan Chen[1*], Qing Xia[1] and Zhuang Li[1]
[1]*Key Laboratory for Anisotropy and Texture of Materials, Ministry of Education, Key Laboratory for Laser Application Technology of Liaoning Province. School of Materials and Engineering, Northeastern University, Shenyang, Liaoning, China*

Keywords: Selective laser melting, Brake disc, 24CrNiMoY steel, Microstructure, Hardness.

Abstract: In this paper, 1.5% ZrO_2 was added in 24CrNiMoY alloy steel powder to form a composite powder, and the alloy steel sample was prepared by selective laser melting technology. Effects of different laser power and scanning speed on the microstructure and hardness of the fabricated sample were studied by OM, XRD, SEM and hardness test. The results show that when the optimized laser power is 1700 W and scanning speed is 10mm/s, the phase structure is composed of martensite, bainite, ferrite and carbide. The microstructure is uniform and fine, there are no cracks in the fabricated sample, the porosity is 0.96%. The average hardness is 467 HV, ZrO_2 plays a role on improving the hardness. The alloy steel sample prepared by SLM has a fine microstructure and high hardness, which provides a basis for laser additive manufacturing of high-speed brake disc.

1 INTRODUCTION

High-speed rail brake discs are one of the key parts that guarantee the safe operation of high-speed rails. Many studies have focused on the manufacturing of brake discs [1, 2]. At present, the rail brake discs are mainly prepared by traditional methods of casting, forging and heat treatment. This method has some problems such as high manufacturing cost, complicated heat treatment process, limited mechanical processing equipment [3]. Selective laser melting is a new technology for the preparation of complex metal parts. It has the characteristics of rapid manufacture, and the structure and performance can be designed and controlled [4, 5]. Therefore, SLM is one of the main research directions to prepare the brake disc with high hardness.

Zirconia is a good reinforcement phase, and its strengthening mechanism has been explored in a variety of papers. Lei et al. [6] used plasma spraying to prepare HA-30% ZrO_2 coating layer. Compared to the pure coatings, microhardness and wear resistance were improved. Gao et al. [7] studied the effect ZrO_2 content on the properties of Cu-ZrO_2 composites. The results show that when the ZrO_2 content was 7%, the hardness and tensile strength are significantly improved. However, the strengthening and toughening mechanism of zirconium oxide in 24CrNiMoY alloy steel has not been studied.

24CrNiMo alloy steel is the main material for the preparation of high-speed rail brake discs, which has the advantages of stable friction characteristics and good wear resistance at high temperature. In our previous studies, the hardness of the 24CrNiMo alloy steel fabricated by SLM technology is 346 HV [8], its hardness is not enough to meet the surface material requirements of brake discs. So we used the vacuum induction melting atomization method to prepare 24CrNiMo steel powder with yttrium added firstly. Then, the laser power and scanning speed was optimized to fabricated 24CrNiMoY steel with ZrO_2. The purpose is to provide a theoretical basis for the preparing of high-speed rail brake discs via SLM.

Table 1: The alloy composition of each element.

element	Fe	C	Cr	Ni	Mo	Mn	O	Si	Y
wt.%	94.74	0.24	0.89	0.937	0.503	0.989	0.02	0.382	1.3

Table 2: Parameters of the fabricated sample process.

Sample Numble	Overlap ratio (%)	Powder thickness (mm)	Spot diameter (mm)	Scanning speed(mm/s)	Power (W)
S1	35	0.4	4	7	1800
S2	35	0.4	4	8	1800
S3	35	0.4	4	9	1800
S4	35	0.4	4	10	1800
S5	35	0.4	4	11	1800
B1	35	0.4	4	10	1600
B2	35	0.4	4	10	1700
B3	35	0.4	4	10	1900
B4	35	0.4	4	10	2000

2 EXPERIMENTAL MATERIALS AND METHODS

2.1 Experimental Materials

The substrate material was Q235 steel. Before the experiment, the surface of Q235 steel plate with dimensions of 100 mm × 100 mm × 10 mm was polished to a roughness of Ra 6.5. The composite powder used for SLM is 24CrNiMoY powder containing 1.5% ZrO_2. The composition of 24CrNiMo powder is shown in Table 1. Composite powder were ball milled using the QM-5 Roller Ball Mill.

2.2 Experimental Methods

The prepared alloy steel powder is uniformly spread on the substrate, and the laser scanning path is controlled to completely melt the powder layer. After each layer is melted, the forming cylinder is lowered by one powder layer thickness, re-powdered and the laser is then completely melted according to a present path. In this experiment, different layers of laser scanning paths were perpendicularly intersected to reduce defects in the laser cladding process. The specific process parameters are shown below.

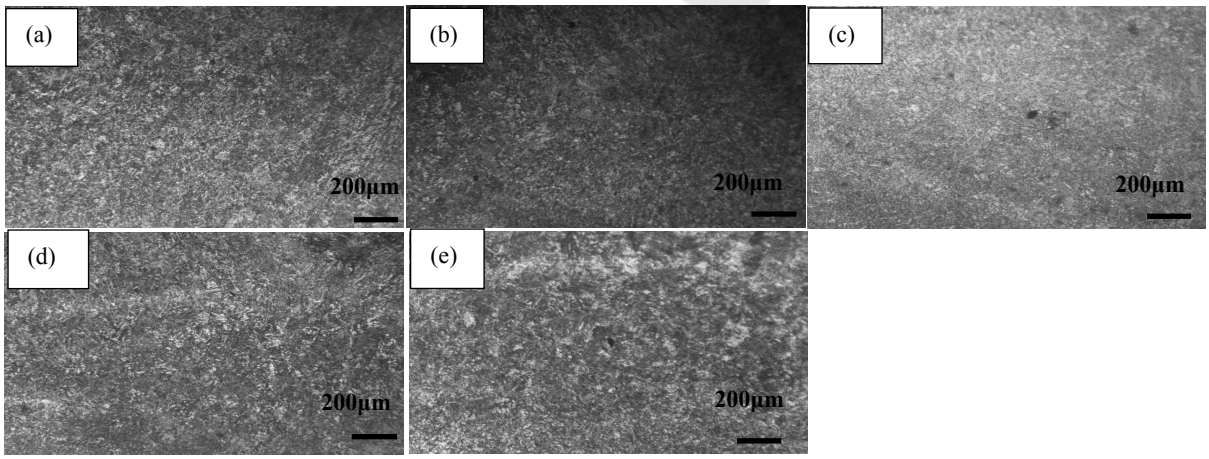

Figure 1: Fabricated sample morphology under different scanning speed. (a) S1 Sample, (b) S2 Sample, (c) S3 Sample, (d) S4 Sample, (e) S5 Sample.

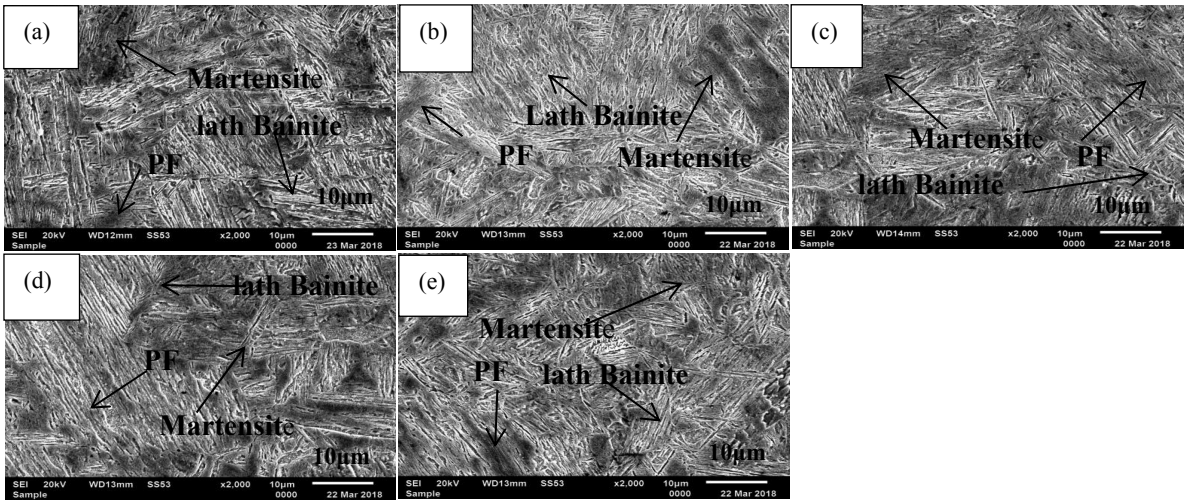

Figure 2. SEM figures of specimens at different laser power. (a) B1 Sample, (b) B2 Sample, (c) S4 Sample, (d) B3 Sample, (e) B4 Sample.

3 EXPERIMENTAL RESULTS AND ANALYSIS

3.1 Effect of Scanning Speed on Microstructure of the Fabricated Sample

Figure 1 shows the metallographic images of the cladding layer at different scanning speeds. It can be seen from the metallographic image that when the power and other process parameters are kept constant, with the change of scanning speed, the number and size of pore defects in the fabricated layer have changed.

3.2 Effect of Power on SEM Pictures of the Fabricated Sample

Figure 2 shows the SEM images of the alloy steel cladding layer under different power. The SEM images show that the phase composition of the cladding layer under different power conditions are martensite, lath bainite and ferrite. During the cooling process of high-temperature austenite, proeutectoid ferrite (PF) grows first at the austenite grain boundary nucleation. Since laser cladding is a rapid cooling process, when austenite is subcooled to the bainite and martensite transformation temperatures, most of the carbon is dissolved in alpha ferrite, so bainite and martensite grows inside austenite crystals.

3.3 Effects of Laser Power and Scanning Speed on Porosity and Hardness of Fabricated Sample

It can be seen from Figure 3 that when the laser power of 1800 W. When the scanning speed is 10mm/s, The porosity of the coating reached a minimum of 1.07%. And at the scanning speed of 10mm/s, when the laser power is 1700 W, the porosity of the fabricated sample reached a minimum of 0.96%.

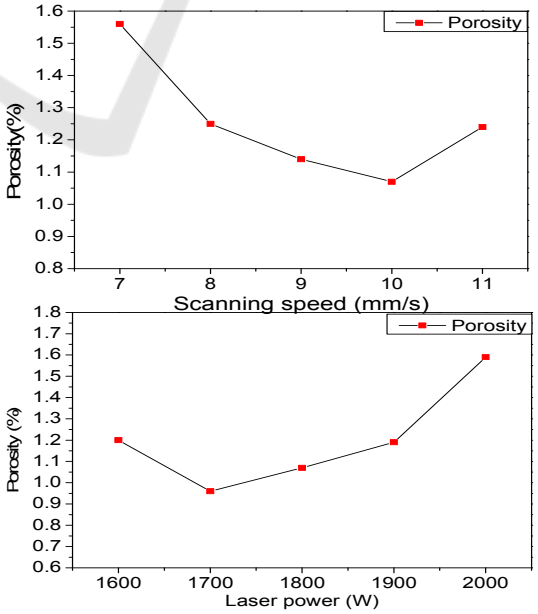

Figure 3: Porosity rate under different scanning speed and laser power.

Figure 4 shows the hardness of the forming layer at different scanning speeds and laser powers. When the laser power is 1800 W, the fabricated sample has the highest hardness when the scanning speed is 10 mm/s, and when the scanning speed is determined as 10 mm/s, With the power of 1700 W, the fabricated sample has the highest hardness.

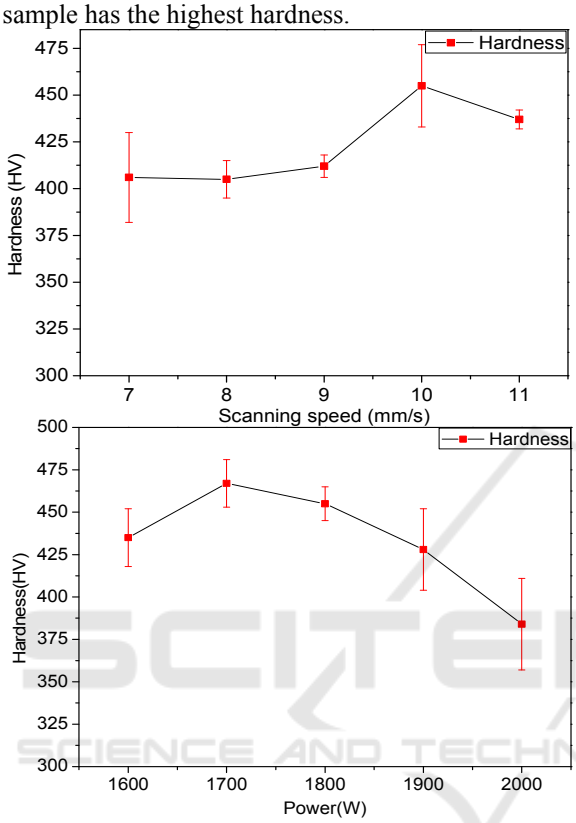

Figure 4: Microhardness of the fabricated sample at different laser power and scanning speed.

Based on the above analysis of the porosity and hardness of the fabricated sample, the optimum power for the SLM process is 1700 W, and the optimal scanning speed is 10 mm/s. The porosity of the fabricated sample under optimal parameters is 0.96% and the hardness is 467 HV.

Figure 5 shows the XRD pattern of the fabricated sample when the laser power is 1700 W and the scanning speed is 10mm/s. It can be seen from the pattern that the main phase of 24CrNiMoY alloy steel is α-Fe(M), and M represents the element C, Cr, Ni, Mo, etc. in the alloy steel. Pre-eutectoid ferrite PF is α-Fe phase with a solid solution carbon content of 0.0218% or less. lath bainite is composed of bainitic ferrite BF phase and carbide phase M_7C_3. Martensite is a supersaturated solid solution of C in α-Fe.The peak of zirconia can also be seen, zirconia is dispersed in the alloy steel as a compound.

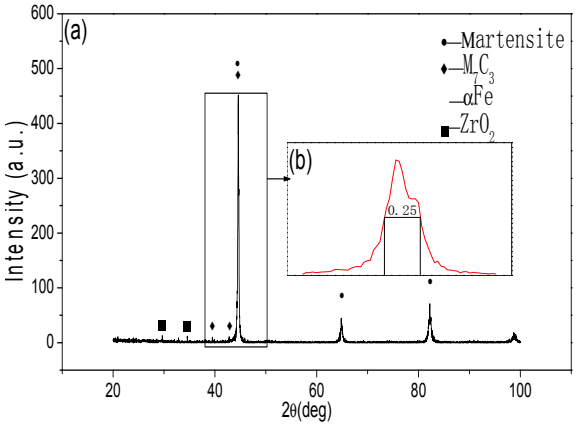

Figure 5: XRD pattern of cladding layer with laser power of 1700 W.

3.4 Analysis and Discussion of Experimental Results

The main process parameters that affect the quality of the fabricated sample include laser power P, scanning speed V, spot diameter D, overlap ratio W, and powder coating thickness H. The energy absorbed per unit volume of the cladding layer is generally expressed according to formula (1).

$$E = \frac{P}{D(1-W)VH} \quad (1)$$

When the laser power is 1600 W, the laser radiation energy is too low, and the energy volume density per unit area of the molten pool is not enough, resulting in insufficient melting of the powder and increasing the probability of generating porosity in the fabricated sample. When the laser power increases to a certain threshold (1700 W in the experiment), as the energy density increases, the depth of the molten pool increases, and the surrounding metal liquid flows to the porosity so that the number of pore is reduced. When the output power of the laser is is too high, a large amount of matrix material will be melted so that the dilution of the alloy of the cladding layer will increase, the stirring of the molten pool will intensify, and the elements of the matrix element and the fabricated sample will mutually diffuse. Resulting in increasing chance of causing porosity.The XRD diffraction peak width can be used to determine the grain size. If the grain size is small, the diffraction direction will be diffused, which cause a broadening of the diffraction peaks [9]. Therefore, the crystal grain size can be judged by the broadening analysis of XRD diffraction peaks.

$$D_{hkl} = \frac{k\lambda}{\beta_{hkl} \cos\theta_{hkl}} \quad (2)$$

The value of k is generally taken as 0.89. It can be seen from formula (2) that the larger the half-height width hkl, the smaller the grain size Dhkl.

Figure 5(b) shows the analysis of the XRD diffraction peaks at a power of 1600 W cladding. In accordance with the same method for the analysis of XRD diffraction peaks at other powers, the results are shown in the table. It can be seen from the table that as the power increases, the half-width of the α-Fe diffraction peak first increases and then decreases, indicating that when the power is from 1700 W to 1800 W, the grain refinement is more obvious.

Table 3: XRD diffraction peak half-height widths of the fabricated sample at different power.

Sample serial number	B1	B2	S4	B3	B4
Laser power	1600	1700	1800	1900	2000
Half-width	0.22	0.25	0.24	0.23	0.22

The grain size under different powers was calculated by Image software. The grain size first decreased with increasing power and then increased, the grain size reaches a minimum at 1700 W. When the laser power is low, the absorbed heat in the molten bath is relatively reduced, the dilution of the fabricated sample is small, and the Fe element of the substrate is less in the cladding layer, so the content of (NiFe) in the cladding layer is low, and the carbide is hard, the higher content of the phase and the tendency to agglomerate to form larger needle-like and strip-like hard phases, as a result of which the grain size of the microstructure increases. Therefore, in a certain range of increasing the laser power, the microstructure of the fabricated sample tends to be dense, and the crystal grains are finer. When the laser power is too large, the solution in the molten pool absorbs more energy and the cooling rate decreases, so that the tissue particles will increase compared to the tissue particles at the moderate scan speed. Which also verifies the the results of statistical analysis using XRD diffraction peak broadening. It can also explain that when the laser power is 1700 W, the grain size refinement is most obvious, and the hardness of the forming layer is the highest.

4 CONCLUSIONS

(1) The 24CrNiMoY alloy steel with ZrO_2 added cladding layer obtained by SLM has good formability, no obvious crack defect, and a small amount of porosity defects. And the defects has a tendency to change as the process parameters change.

(2) When the scanning speed of 10 mm/s and the laser power of 1700 W, the defects of the cladding layer are minimal and the microstructure is uniform, the grain size refinement is most obvious. The grain size is 9.6 μm and the hardness value can reach a maximum value of 467 HV.

(3) By analyzing the SEM images of the cladding layer, it can be concluded that the phase composition of the cladding layer under different power is martensite, bainite and α-ferrite, and the phase composition is uniform.

ACKNOWLEDGEMENTS

This work was financially supported by National Key R&D Program of China (2016YFB1100201), Green Manufacturing System Integration Project of the Industry and Information Ministry of China (2017), Project 201710145047 Supported by National Training Program of Innovation and Entrepreneurship for Undergraduates.Research and development, plan for the future emerging industries in Shenyang(18-004-2-26).

REFERENCES

1. Bartys, H., Guerin, J.D., Watremez, M., Bricout, J.P., 2013 *Surface Engineering.* 17(2) 127-130.
2. Nouby, M., Abdo, J., Mathivanan, D., Srinivasan, K., 2011 *Tribology Transactions.* 54(4) 644-656.
3. Kim, D.J., Seok, C.S., Koo, J.M., We, W.T., Goo, B.C., Won, J.I., 2010 *Fatigue & Fracture of Engineering Materials & Structures.* 33(1) 37-42.
4. Ali, H., Ghadbeigi, H., Mumtaz, K., 2018 *Materials Science & Engineering A.* 712 175–187.
5. Davidson, K., Singamneni, S., 2016 *Materials and Manufacturing Processes.* 31(12) 1543-1555.
6. Fu, L., Khor, K.A., Lim, J.P., 2000 *Surface and Coatings Technology.* 127(1) 66-75.
7. Gao, J., Zheng, J., Li, Q.Y., Hou, C.K., 2006 *Heat Treatment of Metals.* 31(1) 40-42.
8. Shi, C.F., Chen, S.Y., Xia, Q., Li, Z., 2018 *Powder Metallurgy.* 61(1) 73-80.
9. Koker, M.K.A., Welzel, U., Mittemeijer, E.J., 2013 *Philosophical Magazine.* 93(22) 2967-2994.